

# POLARIZED NUCLEI IN A SIMPLE MIRROR FUSION REACTOR

DAVID A. NOEVER *National Aeronautics and Space Administration  
Marshall Space Flight Center, ES76, Huntsville, Alabama 35812*

Received November 29, 1993

Accepted for Publication July 14, 1994

FUSION REACTORS

**KEYWORDS:** *polarized nuclei,  
mirror reactor, alpha particles*

*The possibility of enhancing the ratio of output to input power  $Q$  in a simple mirror machine by polarizing deuterium-tritium (D-T) nuclei is evaluated. Taking the Livermore mirror reference design mirror ratio of 6.54, the expected  $\sin^2 \vartheta$  angular distribution of fusion decay products reduces immediate losses of alpha particles to the loss cone by 7.6% and alpha-ion scattering losses by  $\sim 50\%$ . Based on these findings, alpha-particle confinement times for a polarized plasma should therefore be 1.11 times greater than for isotropic nuclei. Coupling this enhanced alpha-particle heating with the expected  $>50\%$  D-T reaction cross section, a corresponding power ratio for polarized nuclei,  $Q_{\text{polarized}}$ , is found to be 1.63 times greater than the classical unpolarized value  $Q_{\text{classical}}$ . The effects of this increase in  $Q$  are assessed for the simple mirror.*

## INTRODUCTION

The availability of multiampere beams of nuclear polarized atoms<sup>1-3</sup> and their resistance to depolarization under fusion reactor conditions<sup>4-9</sup> has sparked interest in the use of fuel polarization to enhance fusion reactor performance. For a magnetic mirror device, polarization of deuterium (D) and tritium (T) nuclei parallel to the **B** field offers two advantages:

1. a 50% increase in the effective nuclear cross section
2. fusion decay products that are emitted predominantly perpendicular to the magnetic field in a  $\sin^2 \vartheta$  angular distribution.

Because of these two effects, polarization of injected nuclei is expected to increase the ratio of output to input power for the mirror. The higher cross section prom-

ises 50% higher reactivity and 50% more nuclear power for the same conditions (or the same power at lower operating pressures if beta is seriously constrained). Likewise, the  $\sin^2 \vartheta$  angular distribution of generated alpha particles should reduce alpha-particle end losses from the mirror. Consequently, more of the alpha-particle 3520 keV should be deposited in the reactant plasma leading to a net reduction in the required external heating power.

Enhanced alpha-particle trapping results from

1. the reduced number of alpha particles immediately "born" into the loss region
2. the reduced alpha-ion scattering losses of the remaining alpha particles.

For these alpha-particle loss mechanisms, analytical and numerical enhancement factors are derived, and the ratio of polarized to isotropic alpha-particle confinement time is found. These results are incorporated into an equilibrium fusion energy balance to translate the additional alpha-particle heating into a higher ratio of output to input power (henceforth referred to as  $Q$ ).

## ALPHA-PARTICLE HEATING

As larger experimental fusion machines approach reactor conditions, alpha-particle heating is an increasing issue of concern.<sup>10</sup> Alpha particles generated primarily by the reaction  $D + T \rightarrow {}^4\text{He} + n$  carry fully one-fifth of the fusion reaction energy. Since this kinetic energy is "attached" to a charged species, some portion is magnetically confined to be partitioned among the fusion reactants. Alpha-particle studies principally seek to determine the dynamics of energy relaxation within the background plasma and the total amount of energy deposited with each species (see Ref. 11 for summary).

The principal alpha-particle energy loss terms are assumed here to be

1. the immediate loss of alpha particles born into the loss cones
2. slowing-down collisions with electrons and ions
3. pitch-angle scattering by collisions into the loss cones.

Anomalous energy losses such as Alfvén wave coupling will be ignored. Each loss term is considered in turn with the ultimate objective being to develop a simulation model for the energy coupling of the alpha particles to the plasma for both an isotropic and  $\sin^2 \vartheta$  alpha-particle distribution.

### LOSS CONE ALPHA PARTICLES

Ignoring ambipolar potentials, the probability of immediate alpha-particle loss for an isotropic distribution is  $P_{\text{loss}} = 1 - \cos \vartheta_0$ , where  $\cos \vartheta_0 = (1 - R^{-1})^{1/2}$ , and  $R$  is the mirror ratio. Polarized D-T nuclei, on the other hand, have an alpha-particle distribution that is proportional to  $\sin^2 \vartheta_0$  and can be written as

$$\frac{d\sigma}{d\Omega} \sim \sin^2 \vartheta ,$$

valid to the first order in  $d\sigma/d\Omega$ , the fraction of unpolarized nuclei, or as a normalized distribution:

$$P(\Omega) = \frac{3}{8\pi} \sin^2 \vartheta . \quad (1)$$

The probability that an alpha particle is born into the loss cone for polarized D-T nuclei is, therefore,

$$P_{\text{loss}} = \frac{3}{8\pi} \int_0^{2\pi} \int_0^{\vartheta_0} \sin^3 \vartheta_0 d\phi d\vartheta_0 = \int_0^{\Omega_0} P(\Omega) d\Omega ,$$

where  $d\Omega$  is the differential solid angle  $d\Omega = \sin \vartheta d\vartheta d\phi$  or

$$P_{\text{loss}} = 1 - \frac{1}{2} \cos \vartheta_0 (\sin^2 \vartheta_0 + 2) . \quad (2)$$

Table I summarizes the polarized-to-isotropic ratio of trapped alpha particles:

$$\frac{\text{polarized trapped fraction}}{\text{unpolarized trapped fraction}} = \frac{1}{2} (\sin^2 \vartheta_0 + 2) ,$$

which indicates the alpha-particle trapping enhancement by D-T polarization. As expected, the trapping advantage of the distribution increases with loss cone size.

### SLOWING-DOWN AND PITCH-ANGLE SCATTERING

The dynamics of the slowing-down and scattering process is governed by the Fokker-Planck equation, which describes each particle as a material point in seven-dimensional phase and time space. Following the analysis of Sivukhin<sup>12</sup> and Anderson et al.,<sup>13</sup> the

TABLE I  
Polarized-to-Isotropic Ratio of Trapped Alpha Particles

Mirror Ratio	$\Theta$	Isotropic Trapped Fraction	Polarized Trapped Fraction	Ratio of Polarized to Isotropic Trapping
14.9	15	0.97	0.999	1.03
4.0	30	0.87	0.983	1.13
2.0	45	0.71	0.888	1.25
1.3	60	0.50	0.690	1.38
1.1	75	0.26	0.382	1.47

Fokker-Planck equation is written here as an ordinary diffusion equation describing the pitch-angle scattering and solved numerically by standard forward-difference techniques. Anomalous effects of an energy-dependent diffusion coefficient will not be considered.

The following assumptions are made:

1. There is a three-component plasma of Maxwellian electrons and ions with an alpha-particle distribution  $f$  that is isotropic in physical space but arbitrary in velocity space.

2. The alpha-electron scattering can be neglected relative to ion-alpha scattering ( $\sigma \sim v^{-4}$ , which is small for high-velocity electrons).

3. There is a square-well uniform  $\mathbf{B}$  field that runs parallel to the cylindrical mirror axis and rises discontinuously at the ends (thus allowing the mirror field to appear only in the boundary conditions).

4. Only the high-energy end of the alpha-particle distribution (where  $df/dt = 0$  is a valid assumption) is considered.

Using these assumptions, the Fokker-Planck equation takes the form:

$$\frac{1}{v^2} \frac{\partial}{\partial v} (v^2 I_{\parallel}) + \frac{1}{v \sin \vartheta} \frac{\partial}{\partial \vartheta} (v I_{\perp} \sin \vartheta) = S , \quad (3)$$

where  $I_{\parallel}$  and  $I_{\perp}$  are the parallel and perpendicular components of the flux density in velocity space, respectively, and  $S$  is a source function, i.e., the number density of high-energy particles created per second by fusion reactions. Neglecting parallel diffusion relative to the perpendicular flux components (valid for  $v_i \ll v_{\alpha} \ll v_e$ ), Eq. (3) can be written as

$$-\frac{1}{\tau_s v^2} \frac{\partial}{\partial v} [(v^3 + v_c^3)f] - \frac{\kappa}{\tau_s} \frac{v_c^3}{v^3} \frac{\partial}{\partial x} \left[ (1 - x^2) \frac{\partial f}{\partial x} \right] = S , \quad (4)$$

where

$$\frac{1}{\tau_s} = \frac{16}{3} (2\pi)^{1/2} \frac{m_e^{1/2}}{m_\alpha} \frac{e^4 n_e}{(kT_e)^{3/2}} \ln \Lambda$$

$$v_c^3 = (9\pi)^{1/2} \frac{m_e}{m_\alpha} [Z] v_e^3$$

$\tau_s$  = slowing-down time

$v_c$  = critical velocity at which electrons and ions contribute equally to the slowing-down frictional force

$m_e, m_\alpha$  = electron and alpha masses, respectively

$n_e, T_e, e$  = electron density, temperature, and charge, respectively

$\ln \Lambda$  = Coulomb logarithm.

Pitch-angle scattering is described by  $x = v_{\parallel}/v = \cos \vartheta$ , where  $\vartheta$  is the angle between  $\mathbf{v}$  and the  $\mathbf{B}$  axis. The parameters  $\kappa = Z_{eff}/(2A_\alpha[Z])$ ,  $Z_{eff} = \sum Z_i^2 n_i/n_e$ ,  $[Z] = \sum (Z_i^2 n_i/A_i)/n_e$ , and  $A_i$  = mass of the ions ( $A_i$ ) and alpha particles ( $A_\alpha$ ) complete the left-hand side of Eq. (4). The source function,  $S = S_0 \delta(v - v_\alpha) H(x)$  [where  $S_0$  is a constant related to the fusion rate and  $H(x)$  will be given explicitly later] closes the Fokker-Planck description.

Integrating Eq. (4) from  $v_\alpha^-$  to  $v_\alpha^+$  reduces the delta source to the boundary condition:

$$f(v_\alpha^-, x) = \frac{S_0 H(x) v_\alpha^2 \tau_s}{v_\alpha^3 + v_c^3}.$$

Taking the other two boundary conditions as  $f(v, x = \pm x_L) = 0$  for the loss cone space, the problem is well posed. Defining new variables  $\Psi$  and  $t$  as

$$\Psi = (v^3 + v_c^3) f$$

and

$$t = \frac{\kappa}{3} \ln \left( \frac{1 + v_c^3/v^3}{1 + v_c^3/v_\alpha^3} \right), \quad (5)$$

Eq. (4) can be written as

$$\frac{\partial \Psi}{\partial t} = \frac{\partial}{\partial x} \left[ (1 - x^2) \frac{\partial \Psi}{\partial x} \right], \quad (6)$$

with boundary condition

$$\Psi(x, 0) = S_0 v_\alpha^2 \tau_s H(x), \quad |x| \leq x_L$$

and

$$\Psi(\pm x_L, t) = 0, \quad t \geq 0,$$

where  $H(x) = 1$  for an isotropic alpha-particle distribution and  $H(x) = 1 - x^2$  for a  $\sin^2 \vartheta$  distribution.

Numerical solution of Eq. (6) by forward-difference methods [step-size ratio  $\Delta t/(\Delta x)^2 < 0.5$  for stability] gives  $\Psi$  as a function of  $x$  and  $t$ . Using this steady distribution function, the energy spectrum of trapped par-

ticles and the corresponding particle and energy losses can be evaluated for isotropic and  $\sin^2 \vartheta$  alpha-particle distributions. The unnormalized energy spectrum of trapped alpha particles is given by

$$f(v) = \int_0^{x_L} \left[ \frac{\Psi(x, t)}{v^3(t) + v_c^3} \right] dx, \quad (7)$$

and is shown for  $f$  in arbitrary units in Figs. 1 and 2 for both isotropic (ISOT) and polarized (POL) distributions at various mirror ratios. The peak in both distributions around 0.1 contrasts with the standard Maxwellian distribution in that slow alpha particles are preferentially scattered into the loss cones. This altered distribution can be understood to arise directly from the  $1/v^4$  dependence of the Rutherford collision cross section and becomes more pronounced for smaller loss cones.

The particle loss fraction  $P$ , normalized with respect to the total number of generated particles (including those born into the loss cones), is given by

$$P(t) = \frac{\int_0^{x_L} [\Psi(x, 0) - \Psi(x, t)] dx}{\int_0^{x_L} \Psi(x, 0) dx}.$$

Particle loss fraction as a function of energy during slowdown for both isotropic and  $\sin^2 \vartheta$  initial distributions in a 10-keV D-T plasma is shown in Fig. 3 for mirror ratios of 2 and 10.

The energy fraction  $Q$  was found in terms of this particle loss fraction by

$$Q[P(t)] = \int_0^P \frac{v^2(t)}{v_\alpha^2} dP \quad \text{for } 0 \leq P \leq 1$$

and is shown in Fig. 4 for mirror ratios of 2 and 10.

A total energy-scattering rate for the isotropic and  $\sin^2 \vartheta$  alpha-particle distribution was found to be  $\sim 6$  and  $2\%$ , respectively, for a mirror ratio of 10, and 12 and  $5\%$ , respectively, for a mirror ratio of 2. The results for the isotropic alpha-particle case are in good agreement with the findings of Anderson et al.,<sup>13</sup> reported as 6 and  $10\%$  for  $R = 10$  and  $R = 2$ , respectively. Based on this analysis, injection of polarized D-T nuclei has the potential to reduce alpha-particle scattering losses by  $50\%$  or more. However, given that losses are responsible for negligible alpha-particle energy leakage, little improvement in overall  $Q$  can be expected from this reduction.

## ALPHA-PARTICLE CONFINEMENT TIMES

To find an analytic expression for the ratio of polarized to isotropic alpha-particle confinement times, a quasi-Maxwellian distribution function is assumed,

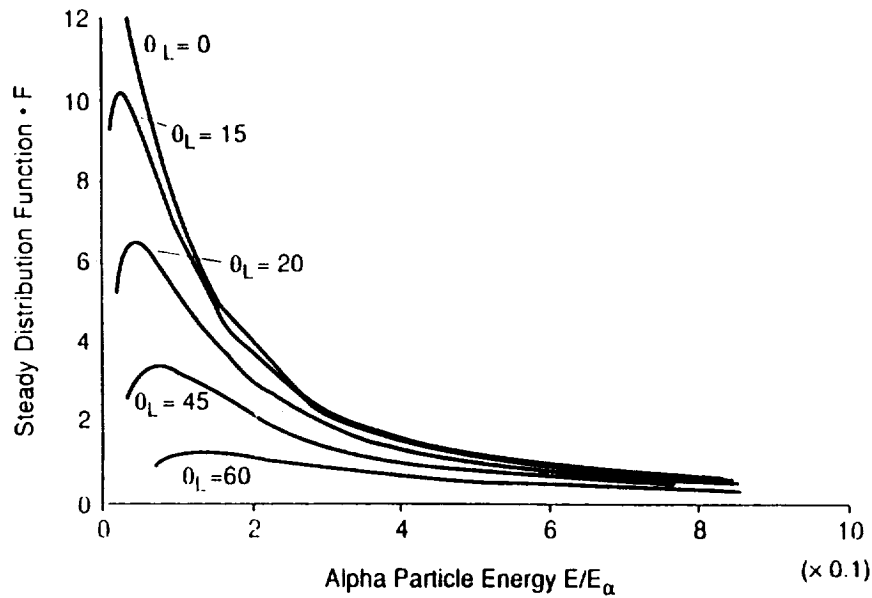


Fig. 1. Effect of end loss on isotropic steady distribution function.

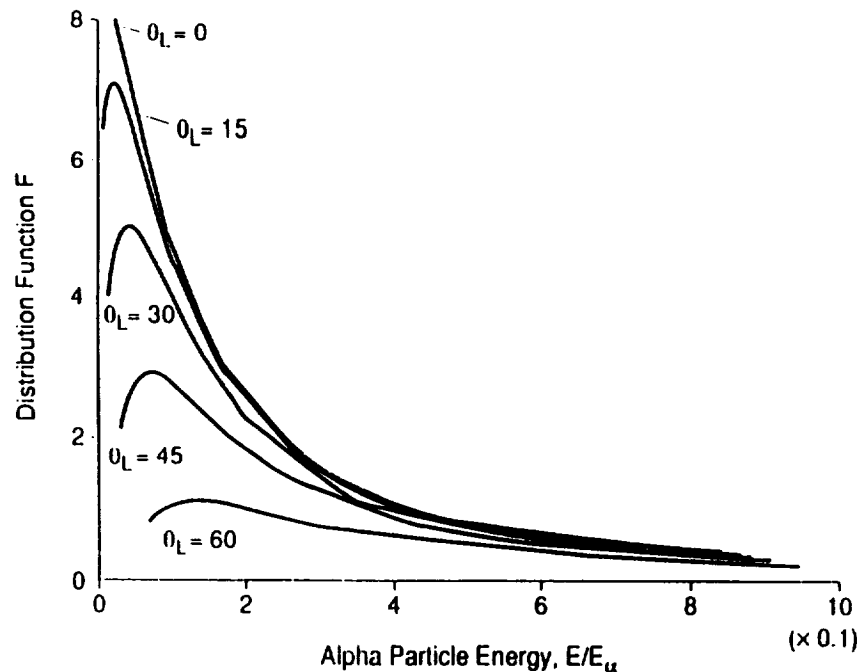


Fig. 2. Effect of end loss on polarized steady distribution function.

and Eq. (3) is solved to give the alpha-particle loss rates. While on first inspection, the assumption of Maxwellian alpha-particle behavior may seem artificial, Galbraith and Kammash<sup>14</sup> found a <1% difference in the key parameter for this investigation, alpha-ion fractional heating, for a Maxwellian over a mirror alpha-particle distribution. Therefore, given the complications

of a full Fokker-Planck calculation, such a simplifying assumption seems justified for the purposes of this investigation.

Equation (3) translated to  $(p, \vartheta)$  space is

$$p \frac{\partial}{\partial \vartheta} (\sin \vartheta I_{\vartheta}) + \sin \vartheta \frac{\partial}{\partial p} (p^2 I_p) = qp^2 \sin \vartheta, \quad (8)$$

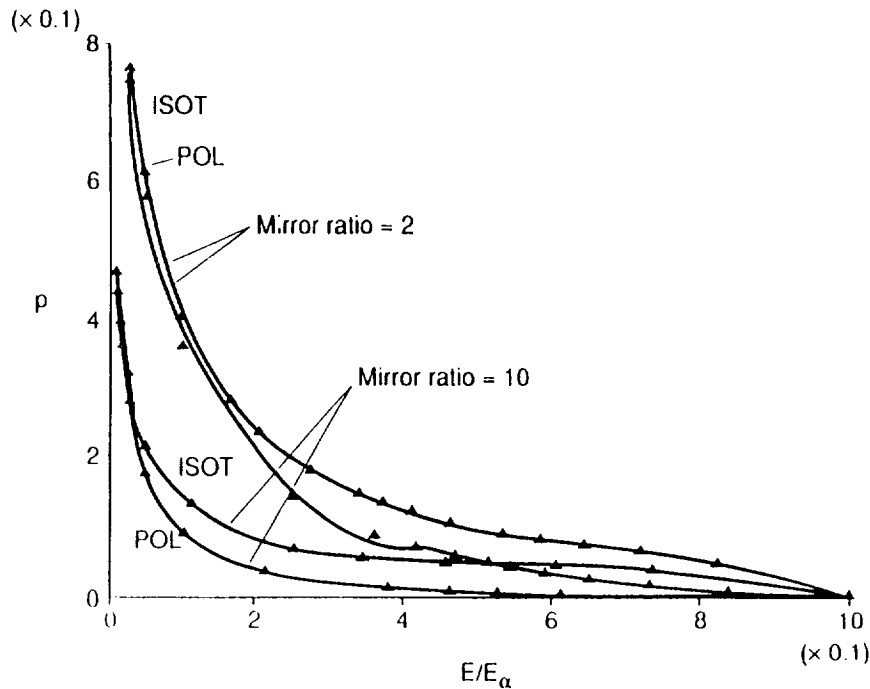


Fig. 3. Particle loss fraction versus alpha-particle energy.

where  $q$  is the source density of alpha particles and  $I_p$  and  $I_\vartheta$  are the momentum and angular flux components, respectively. Following Sivukhin,<sup>12</sup>

$$I_\vartheta = \frac{1}{p} D_{\vartheta\vartheta} \frac{\partial F}{\partial \vartheta} - D_{\vartheta p} \frac{\partial F}{\partial p} + A_\vartheta F,$$

$$I_p = -D_{pp} \frac{\partial F}{\partial p} - \frac{1}{p} D_{p\vartheta} \frac{\partial F}{\partial \vartheta} + A_p F,$$

and

$$D_{\vartheta p} = D_{p\vartheta}.$$

As before, the distribution function vanishes at the loss cone boundary,  $F = 0$  for  $\vartheta = \vartheta_0$ , and by symmetry,  $\partial F / \partial \vartheta = 0$  for  $\vartheta = \pi/2$ .

Since an exact solution requires knowledge of both the diffusion tensor  $D_{\alpha\beta}$  and the coefficient of dynamical friction  $A$  to find the unknown distribution function, the diffusion approximation is employed. By replacing  $D_{\alpha\beta}$  and  $A$  by known functions of  $p$  and  $\vartheta$ , as if  $F$  were isotropic,  $D_{p\vartheta}$  and  $A_\vartheta$  vanish. Furthermore,  $D_{pp} = D_\parallel$ ,  $D_{\vartheta\vartheta} = D_\perp$ , and  $A_p = A$  and are all functions of  $p$  only. Equation (8) can then be written as

$$D_\perp \frac{\partial}{\partial \vartheta} \left( \sin \vartheta \frac{\partial F}{\partial \vartheta} \right) + \sin \vartheta \frac{\partial}{\partial p} \left[ p^2 \left( D_\parallel \frac{\partial F}{\partial p} - AF \right) \right] = -qp^2 \sin \vartheta. \quad (9)$$

Since a quasi-Maxwellian distribution function is sought,

$$F(p, \vartheta) = \Theta(\vartheta) \exp \left( \frac{-p^2}{2mT} \right). \quad (10)$$

Equation (9) simply reduces to

$$\frac{\partial}{\partial \vartheta} \left( \sin \vartheta \frac{\partial F}{\partial \vartheta} \right) = \frac{-qp^2}{D_\perp} \sin \vartheta, \quad (11)$$

which, when coupled with the boundary conditions, gives

$$F = \frac{qp^2}{D_\perp} \ln \frac{\sin \vartheta}{\sin \vartheta_0}.$$

Comparing this result with Eq. (10) gives

$$\Theta = C \ln \frac{\sin \vartheta}{\sin \vartheta_0}$$

or

$$F = C \ln \frac{\sin \vartheta}{\sin \vartheta_0} \exp \left( \frac{-p^2}{2mT} \right),$$

where the normalization constant  $C$  is found from the particle conservation requirement,

$$n = \int F(\vartheta, p) dp. \quad (12)$$

Since an equilibrium alpha-particle loss term is desired, the number of alpha particles lost should equal the number produced, or

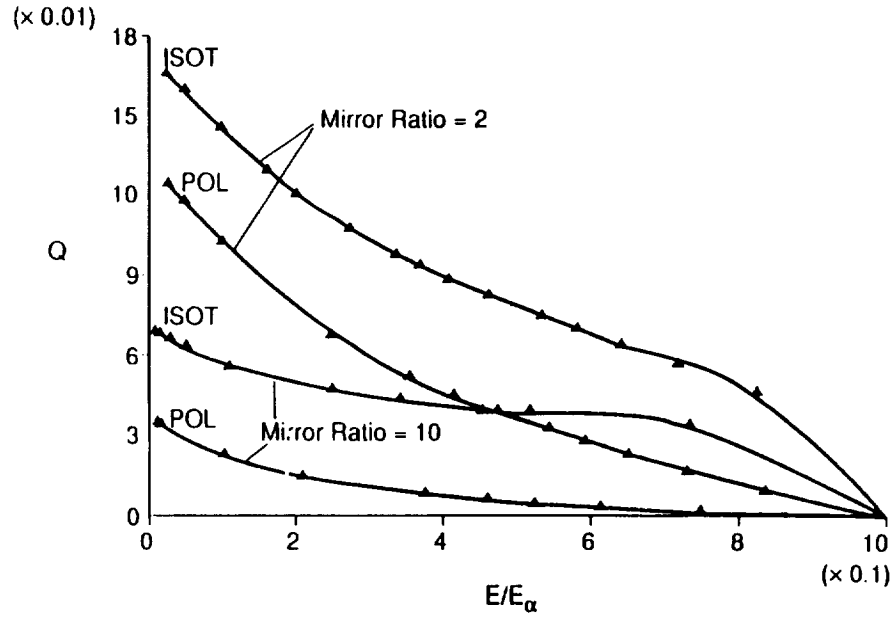


Fig. 4a. Energy loss fraction versus alpha-particle energy.

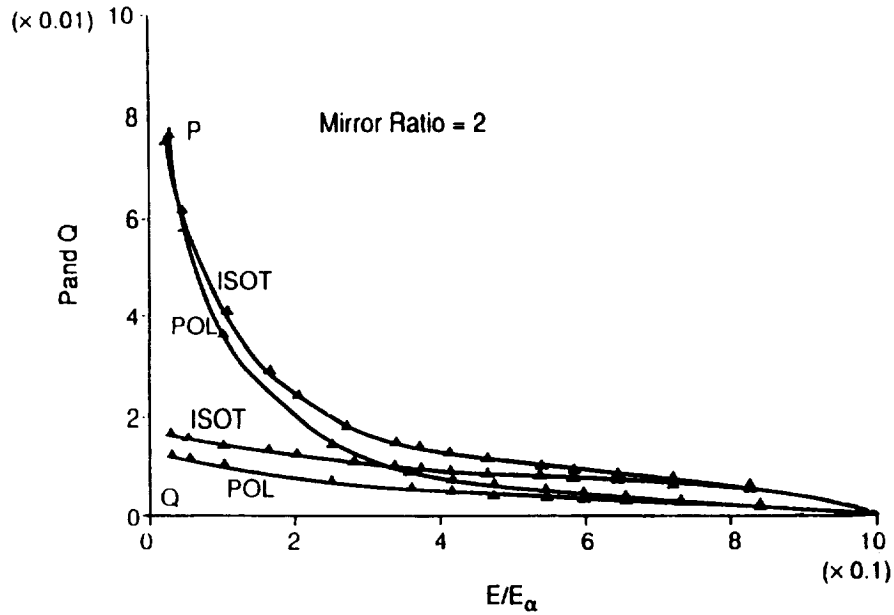


Fig. 4b. Particle and energy loss fractions versus alpha-particle energy.

$$N = \int_{\vartheta_0 < \vartheta < \pi - \vartheta} q dp, \quad (13)$$

where the vector  $d\mathbf{p} = 2\pi p^2 \sin^2 \vartheta d\vartheta dp$ .

For an isotropic alpha-particle distribution,  $\Theta(\vartheta) = 1$ ,

$$n = 2\pi C \int_{\vartheta_0}^{\pi - \vartheta_0} \ln \frac{\sin \vartheta}{\sin \vartheta_0} \sin \vartheta d\vartheta \\ \times \int_0^\infty p^2 \exp\left(\frac{-p^2}{2mT}\right) dp$$

or

$$C = \frac{n}{(2\pi mT)^{3/2} \left[ \ln \left( \cot \frac{\vartheta_0}{2} \right) - \cos \vartheta_0 \right]},$$

such that the loss rate (13) is

$$N = \left( \frac{2\pi}{m} \right)^{1/2} \frac{\ln \Lambda e^4 n^2}{T^{3/2}} \frac{3 \ln(\sqrt{2} + 1) - \sqrt{2}}{\ln \left( \cos \frac{\vartheta_0}{2} \right) - \cos \vartheta_0} \cos \vartheta_0.$$

For a polarized alpha-particle source term, on the other hand,  $q = q_0(p)\Psi(\vartheta)$ , where  $\Psi(\vartheta)$  is normalized to give the same value for  $q$  as for the case of isotropic alpha particles [ $\Psi(\vartheta) = 1$ ]:

$$\int_{\vartheta_0}^{\pi/2} \Psi(\vartheta) \sin \vartheta d\vartheta = \cos \vartheta_0,$$

$$\begin{aligned} \frac{\tau_{pol}}{\tau_{iso}} &= \frac{\frac{1}{1 - (\frac{1}{3})\cos^2 \vartheta_0} \int_{\vartheta_0}^{\pi/2} \left[ \frac{2}{3} \ln \frac{\sin \vartheta}{\sin \vartheta_0} - \frac{1}{6} (\cos^2 \vartheta - \cos^2 \vartheta_0) \right] \sin \vartheta d\vartheta}{\int_{\vartheta_0}^{\pi/2} \sin \vartheta \ln \frac{\sin \vartheta}{\sin \vartheta_0} d\vartheta} \\ &= \frac{\frac{2}{3} \left[ \frac{1}{1 - (\frac{1}{3})\cos^2 \vartheta_0} \right] \left[ \ln \left( \cot \frac{\vartheta_0}{2} \right) - \cos \vartheta_0 + \frac{1}{6} \cos^3 \vartheta_0 \right]}{\ln \left( \cot \frac{\vartheta_0}{2} \right) - \cos \vartheta_0}. \end{aligned} \quad (15)$$

where  $\Psi(\vartheta) = K \sin^2 \vartheta$  gives

$$\Psi(\vartheta) = \frac{\sin^2 \vartheta}{1 - (\frac{1}{3})\cos^2 \vartheta_0}. \quad (14)$$

Solving Eq. (11) for  $F$  as before gives

$$F = \frac{q_0 p^2}{D_{\perp}} \int_{\vartheta_0}^{\vartheta'} \frac{d\vartheta'}{\sin \vartheta'} \int_{\vartheta'}^{\pi/2} \Psi(\vartheta'') \sin \vartheta'' d\vartheta''$$

and

$$F = \frac{q_0 p^2}{D_{\perp} \{1 - (\frac{1}{3})\cos^2 \vartheta_0\}} \times \left[ \frac{2}{3} \ln \frac{\sin \vartheta}{\sin \vartheta_0} - \frac{1}{6} (\cos^2 \vartheta - \cos^2 \vartheta_0) \right].$$

Comparing this again with the quasi-Maxwellian form gives a  $\Theta$  dependence of

$$\begin{aligned} \Theta(\vartheta) &= \frac{C}{1 - (\frac{1}{3})\cos^2 \vartheta_0} \\ &\times \left[ \frac{2}{3} \ln \frac{\sin \vartheta}{\sin \vartheta_0} - \frac{1}{6} (\cos^2 \vartheta - \cos^2 \vartheta_0) \right]. \end{aligned}$$

Because of the previous normalization of the source term, the alpha-particle loss rate  $N$  is the same for

both isotropic and polarized alpha-particle distributions [Eq. (14)], and the difference in confinement times  $\tau = n/N$  is found in the normalization [Eq. (12)]. Instead of

$$\int_{\vartheta_0}^{\pi/2} \sin \vartheta \ln \frac{\sin \vartheta}{\sin \vartheta_0} d\vartheta$$

for the isotropic distribution, the polarized integral is

$$\begin{aligned} &\frac{1}{1 - (\frac{1}{3})\cos^2 \vartheta_0} \\ &\times \int_{\vartheta_0}^{\pi/2} \left[ \frac{2}{3} \ln \frac{\sin \vartheta}{\sin \vartheta_0} - \frac{1}{6} (\cos^2 \vartheta - \cos^2 \vartheta_0) \right] \\ &\times \sin \vartheta d\vartheta. \end{aligned}$$

Based on this analysis, the ratio of alpha-particle confinement is

Figure 5 summarizes these results for various mirror ratios. As expected, Eq. (15) approaches 1 in the limit as the loss cone goes to  $\frac{\pi}{2}$  and  $\pi/2$ . Figure 6 uses an approximation formula<sup>15</sup> for alpha-particle slowing-down behavior to demonstrate the effect of this enhanced alpha-particle confinement on the deposited plasma energy.

## FUSION ENERGY BALANCE

To assess the impact of this enhanced alpha-particle trapping on calculated  $Q$  values, an equilibrium ion and electron energy balance is performed. Following Kam-mash,<sup>16</sup> the ion and electron injection power per unit volume is  $W_{si}$  and  $W_{se}$ , respectively. The geometric confinement time is  $\tau_i$  and  $\tau_e$  for ions and electrons, and when they escape, they carry  $W_{Li}$  and  $W_{Le}$ .

The term  $W_{ij}$  is taken here as the energy exchange between each species ( $W_{ij} = 0$  for  $i = j$ ). With these definitions, the ion energy balance can be written as

$$\frac{d}{dt} (\frac{3}{2} n_i T_i) = 0 = W_{i\alpha} + W_{si} + W_{Li} - W_{ei},$$

where

$$W_{i\alpha} = \frac{1}{4} n_i^2 \langle \sigma v \rangle U_{i\alpha} \quad (\text{keV/m}^3 \cdot \text{s}).$$

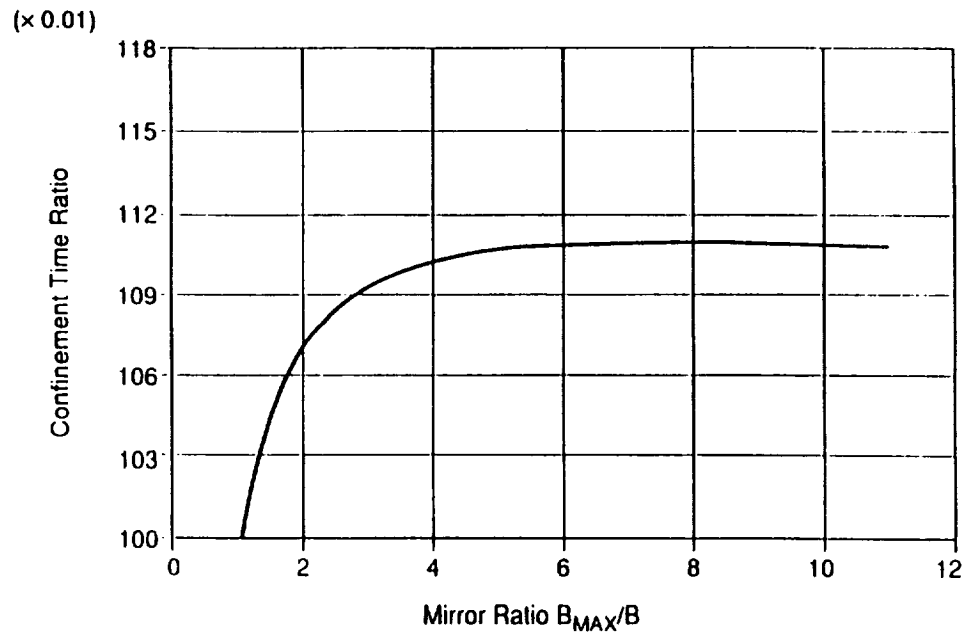


Fig. 5. Alpha-particle confinement times versus mirror ratio.

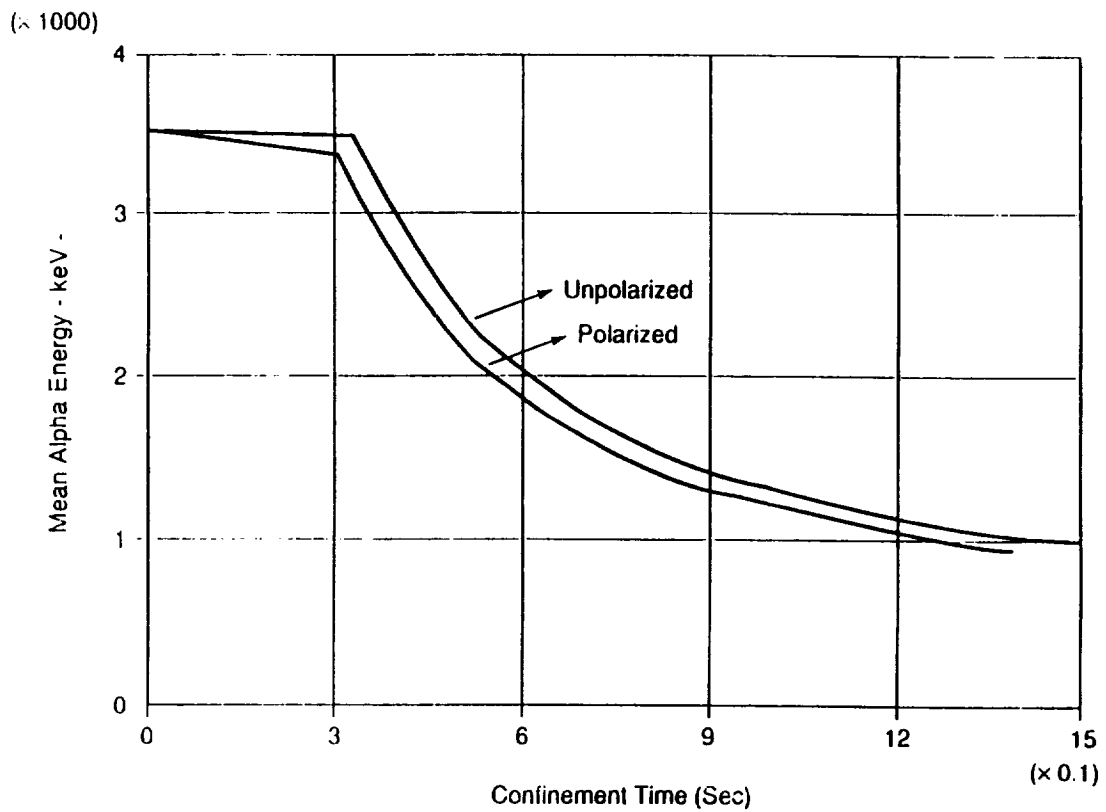


Fig. 6. Mean alpha-particle energy during slowdown.



If  $U_{i\alpha}$  is that portion of the alpha-particle energy deposited with the ions, then

$$W_{si} = S_i V_i = V_i \left( \frac{n_i}{\tau_i} + \frac{n^2 \langle \sigma v \rangle}{4} \right) \quad (\text{keV/m}^3 \cdot \text{s}).$$

If the source  $S_i$  = ion loss rate and  $\tau_s$  = thermalization time, then

$$W_{ei} = \frac{d}{dt} \left( \frac{3}{2} n_i T_i \right)_{\text{exchange}} = \frac{3}{2} \frac{n_i T_i}{\tau_s} \left( 1 - \frac{T_e}{T_i} \right)$$

and

$$W_{Li} = \left( \frac{3}{2} S_i T_i \right)_{\text{exchange}} = \frac{3}{2} T_i \left( \frac{n}{\tau_i} + \frac{n^2 \langle \sigma v \rangle}{4} \right) \quad (\text{keV/m}^3 \cdot \text{s}).$$

Combining these effects, the ion energy balance is

$$\langle \sigma v \rangle (2U_{i\alpha} + 2V_i - 3T_i) \frac{(12T_i - 8V_i)}{n\tau_i} - \frac{9.6 \times 10^{-18}}{T_e^{3/2}} T_i \left( 1 - \frac{T_e}{T_i} \right) = 0. \quad (16)$$

Similarly, the electron energy balance can be written

$$\frac{d}{dt} \left( \frac{3}{2} n_e T_e \right) = 0 \\ = W_{\alpha e} + W_{se} + W_{ei} - W_{Le} - W_x - W_c,$$

where

$$W_{\alpha e} = \frac{n^2}{4} \langle \sigma v \rangle U_{\alpha e} \quad (\text{keV/m}^3 \cdot \text{s}).$$

If  $U_{\alpha e}$  is that portion of the alpha-particle energy (keV/m<sup>3</sup>·s) deposited with the electrons, then

$$W_{se} = V_e \left( \frac{n_e}{\tau_e} + \frac{n^2 \langle \sigma v \rangle}{4} \right),$$

$$W_{ei} = 1.2 \times 10^{-18} \frac{n^2 T_i}{T_e^{3/2}} \left( 1 - \frac{T_e}{T_i} \right),$$

$$W_{Le} = \frac{3}{2} n_e T_e = \frac{3}{2} T_e \left( \frac{n_e}{\tau_e} + \frac{n^2 \langle \sigma v \rangle}{4} \right),$$

and

$$W_x = C_1 \frac{3}{2} n_e \frac{dT_e}{dt} = (3 \times 10^{-21}) C_1 n^2 T_e^{1/2},$$

where  $C_1$  is an adjustable parameter to account for changing bremsstrahlung,

$$W_c = 6 \times 10^{-28} C_2 n^2 T_e^{11/4} (T_e + T_i)^{3/2} \left( 1 - \frac{T_e}{204} \right) / D \quad (\text{keV/m}^3 \cdot \text{s}),$$

and analogously for including a  $C_2$  to account for reflectivity of synchrotron radiation from the wall with a dimensional size parameter

$$D = \beta^{3/2} (LB)^{1/2}.$$

The electron energy balance simplifies to

$$\langle \sigma v \rangle (2U_{i\alpha} + 2V_e - 3T_e) - (12T_e - 8V_e)/n\tau_e + \frac{9.6 \times 10^{-18}}{T_e^{3/2}} T_i \left( 1 - \frac{T_e}{T_i} \right) - 4.8 \times 10^{-27} C_2 T_e^{11/4} (T_e + T_i)^{3/2} \times \left( 1 + \frac{T_e}{204} \right) / D = 0. \quad (17)$$

Combined, Eqs. (16) and (17) form a nonlinear set with roots equal to the equilibrium ion and electron temperature if the following quantities are specified:

1. ion and electron injection energies  $V_i, V_e$
2. burnup fraction  $f_L = (S_i - L_i)/S = (1 + [4/\langle \sigma v \rangle \langle n\tau \rangle])^{-1}$
3. ratio of ion to electron confinement times ( $\tau_i/\tau_e$ ) =  $\gamma$
4. bremsstrahlung parameter  $C_1$
5. synchrotron radiation reflection adjustment  $C_2$
6. size parameter  $D$ .

Equations (16) and (17) were solved using a two-dimensional Newton-Raphson iterative scheme in  $(T_i, T_e)$  space with the cross-section data called from an interpolating subroutine for the smoothed Glasstone-Lovberg<sup>17</sup> results. For comparison sake, relevant machine parameters were taken from the Livermore mirror reference design<sup>18</sup> (LMRD) and are summarized in Table II.

Figures 7 and 8 show equilibrium temperatures versus burnup fraction for both polarized and unpolarized fuel injection. As expected, polarized nuclei elevate both the equilibrium ion and electron temperatures with the more substantial energy gain found in electron temperatures due to preferential alpha-electron energy exchange. The relevant ratio for  $Q$  calculations, however, is the ratio of ion energies, which is shown versus burnup fraction in Fig. 9.

## Q CALCULATIONS

A useful parameter for evaluating mirror reactor machines is  $Q$ , the ratio of fusion power per unit volume ( $P_F$ ) to the power per unit volume injected and trapped in the plasma ( $P_{in}$ ). In turn,  $P_{in}$  is related to the beam energy  $E_{in}$ , and the equivalent injected current by the expression  $P_{in} = E_{in} I_{in}$ . For steady-state

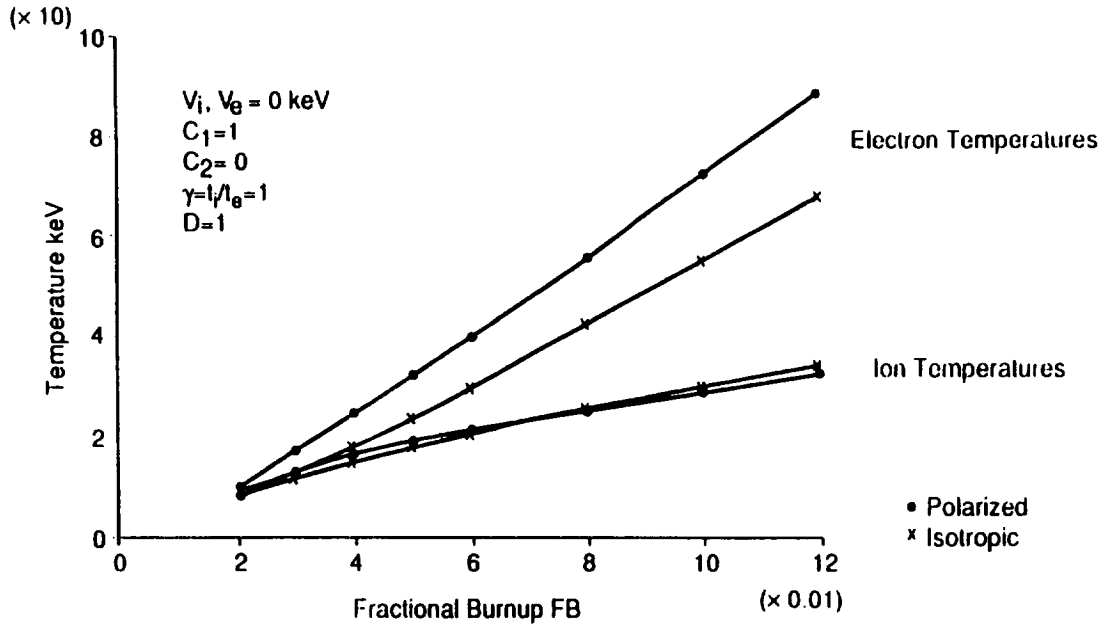


Fig. 7. Equilibrium temperature for isotropic and polarized alpha-particle distributions as a function of fractional burnup.

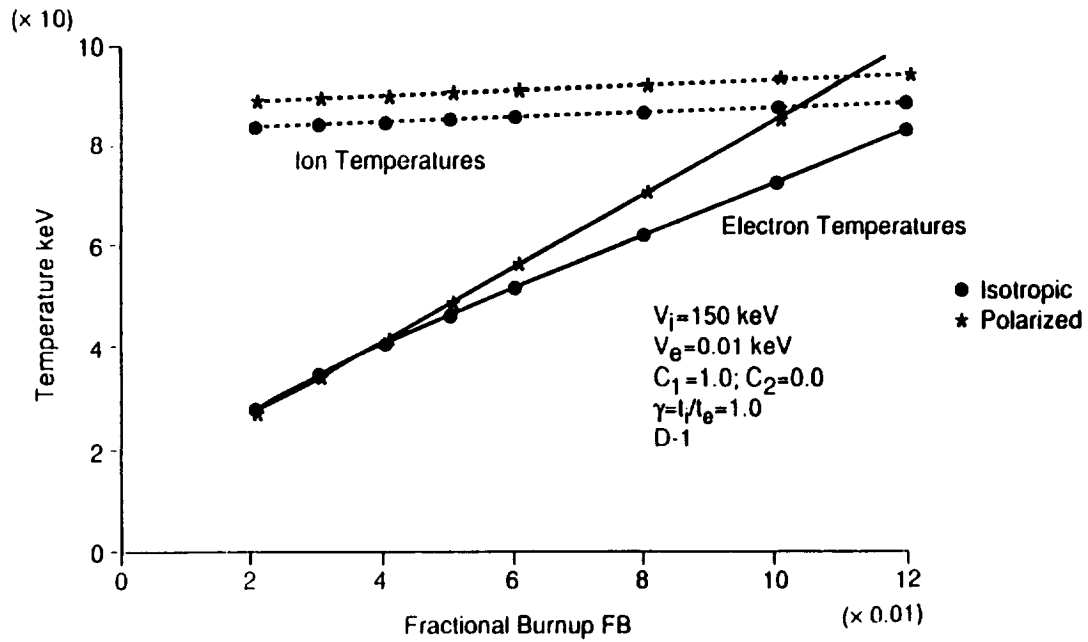


Fig. 8. Equilibrium temperature for isotropic and polarized alpha-particle distributions as a function of fractional burnup.

operation, the input current must equal the rate of particle losses given by

$$I_{out} = \int \frac{n}{\tau} dV = \int \frac{n^2}{n\tau} dV ,$$

where  $n$  is the ion density and  $\tau$  is the mean confinement time, or

$$P_{in} = E_{in} \int \frac{n^2}{n\tau} dV = \frac{E_{in}}{\langle n\tau \rangle} \int n^2 dV .$$

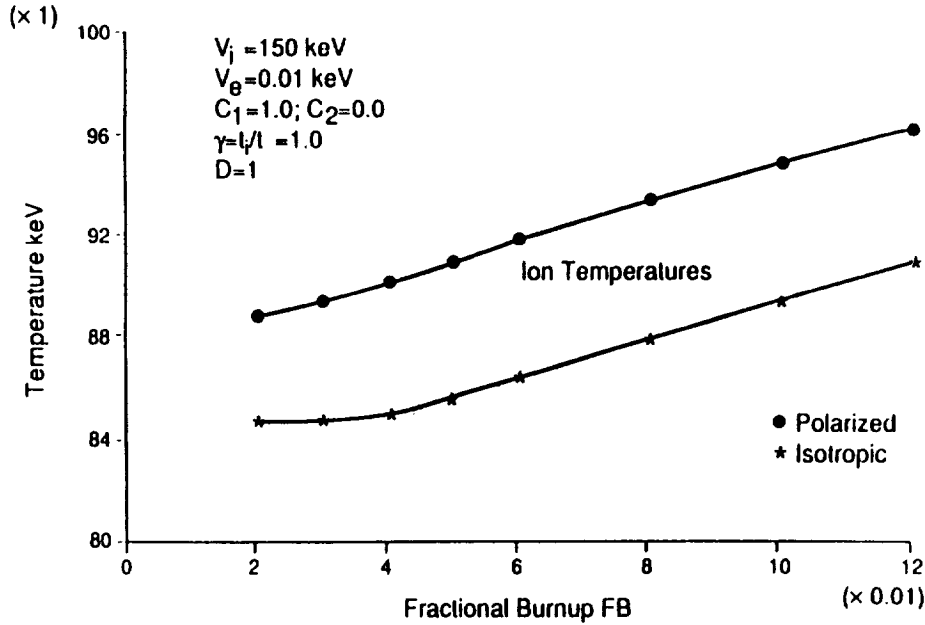


Fig. 9. Equilibrium ion temperature for isotropic and polarized alpha-particle distributions as a function of fractional burnup.

Likewise, since

$$P_F = \frac{\langle \sigma v \rangle E_F}{4} \int n^2 dV ,$$

for a 50-50 D-T plasma,  $Q$  can be written as

$$Q = \frac{\langle n\tau \rangle \langle \sigma v \rangle E_F}{4E_{in}} ,$$

neglecting the differences in  $\langle \sigma v \rangle$  and  $E_{in}$  for deuterium and tritium.

Previous mirror feasibility studies<sup>18</sup> have arrived at a reference design values for a mirror  $Q$  of 1.20 with 77% of the gross electrical power recirculated, a number substantially below the economically attractive range of 3 to 5 for  $Q$ . However, given the fact that modest improvements in  $Q$  can reduce significantly the cost of power, various methods for  $Q$  enhancement are being investigated (see Ref. 19 for summary). In the study of enhanced  $Q$  devices, the functional dependence of the classical  $Q$  predicted by the complete Fokker-Planck calculations is retained, but  $Q_{enhanced}$  is found by multiplying  $Q_{classical}$  by some constant factor. More specifically, since numerous investigations have concluded that for a fixed injection energy and angle,

$$\langle n\tau \rangle \sim E^{3/2} \log_{10} R ,$$

where  $E$  is the mean ion energy and  $R$  is the effective mirror ratio;  $Q_{pol}/Q_{isotropic}$  can be written for cases of interest as

$$\frac{Q_{polarized}}{Q_{isotropic}} = \frac{\langle n\tau \rangle_{enhanced} \langle \sigma v \rangle_{enhanced}}{\langle n\tau \rangle_{classical} \langle \sigma v \rangle_{classical}} = \left( \frac{E_{enhanced}}{E_{classical}} \right)^{3/2} \frac{\langle \sigma v \rangle_{enhanced}}{\langle \sigma v \rangle_{classical}} , \quad (18)$$

where the right-hand side of Eq. (18) is the multiplicative factor desired for a particular design.

TABLE II  
Reference Mirror Parameters

Physics Parameters	Engineering Parameters
Mirror ratio = 6.54 $P_C = 3.52$ keV $P_N = 14.1$ M keV 91% alpha trapping $\langle \sigma v \rangle_\alpha = 7.57 \times 10^{-16}$ cm <sup>3</sup> /s $Q = 1.20$	$V_i = 150$ keV $V_e = 0.01$ keV $M = 1.68$ Injector efficiency = 0.80 DC efficiency = 0.76 Thermal efficiency = 0.50
Unpolarized injection $U_{ae} = 2242$ keV $U_{ai} = 416$ keV Polarized injection $U_{ae} = 2681$ keV $U_{ai} = 487$ keV Alpha trapping enhancement = 1.09	

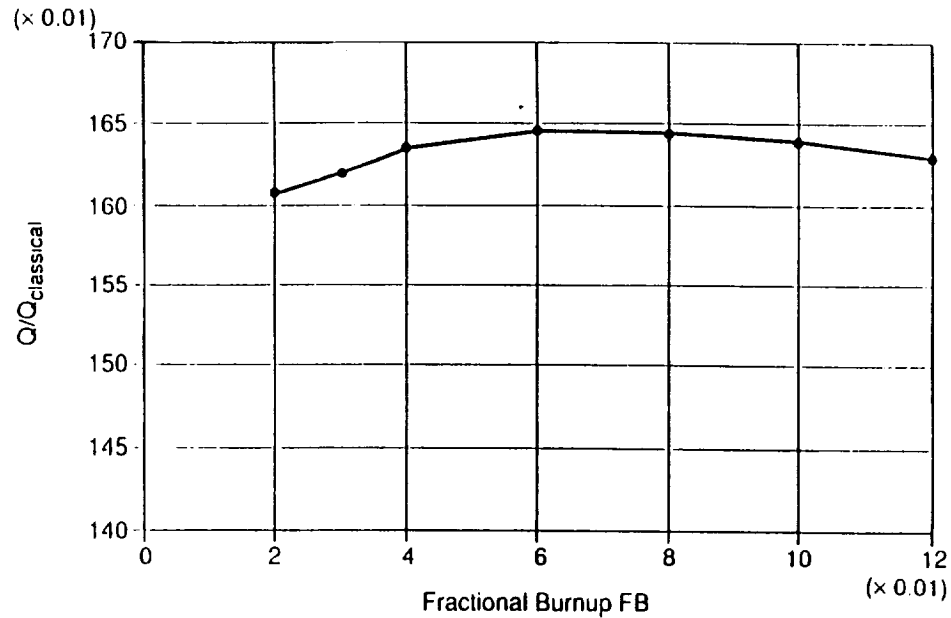


Fig. 10.  $Q/Q_{\text{classical}}$  for polarized plasma in a simple mirror.

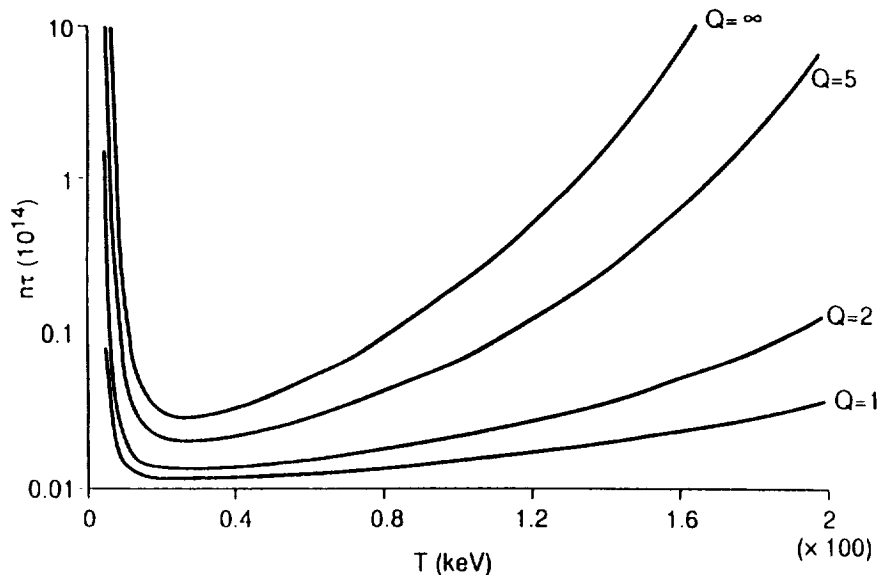


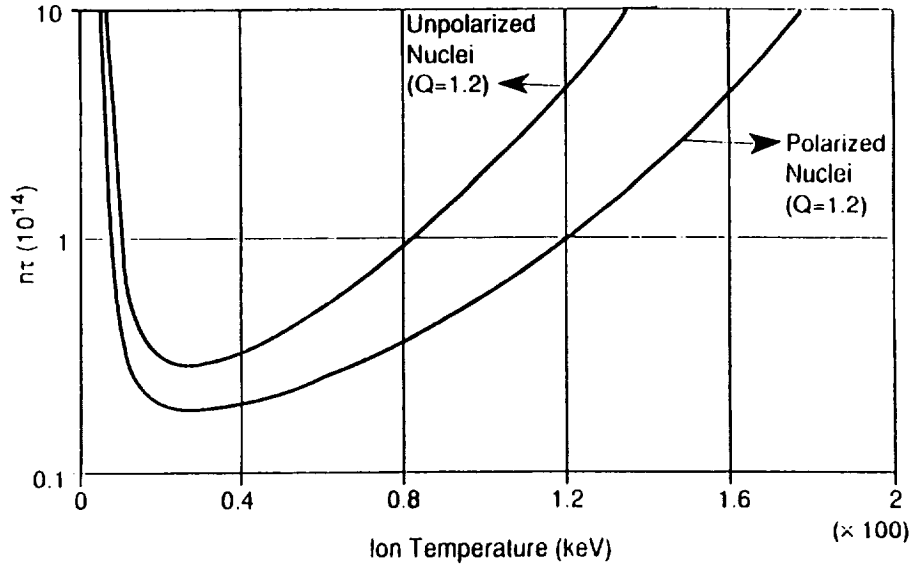
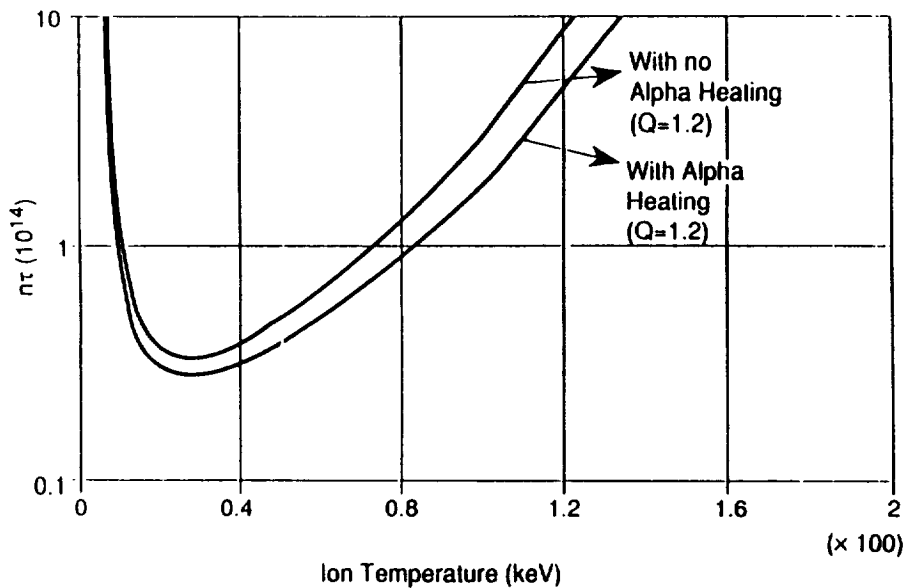
Fig. 11.  $Q$  contours for D-T reactor.

For a simple mirror fueled with polarized nuclei, both the  $<50\%$  reaction index and the higher mean ion energy should enhance expected  $Q$  values. The ratio  $Q_{\text{polarized}}/Q_{\text{classical}}$  is shown in Fig. 10 for various fractional burnup rates. For the LMRD parameters, a  $Q$  enhancement factor of 1.63 is found here. The impact of this  $Q$  enhancement on  $n\tau$  requirements is shown in Figs. 11 and 12.

## DISCUSSION

### System Efficiency

Here,  $Q$  is chosen as the reactor parameter of interest because it simply displays the breakeven  $Q = 1$  and because it can be written in terms of general physics specifications. For operating power plants, however,


 Fig. 12a. Effect of polarization on  $n\tau$  requirements.

 Fig. 12b. Effect of alpha-particle heating on  $Q$  contours.

the overall thermal efficiency may prove more useful. This overall efficiency is defined as the ratio of usable power to fusion power, or  $\epsilon = P_{net}/P_F$ . Decomposing the power terms as shown in the flow diagram of Fig. 13 and neglecting radiation and auxiliary power terms, the efficiency can be written in terms of  $Q$  as

$$\epsilon = \frac{\xi_i}{1 + \frac{P_C}{P_N}} + \frac{(P_C/P_N)\xi_{DC}}{1 + \frac{P_C}{P_N}} - \frac{1 - \xi_i\xi_{DC}}{\xi_i Q},$$

where  $P_C/P_N$  is the ratio of total power in charged species to neutral species and  $\xi_i$ ,  $\xi_{DC}$ ,  $\xi_i$  are the operating efficiencies of the thermal converter, the direct converter, and the injector, respectively. Substituting the LMRD mirror parameters, Fig. 14 summarizes the effect of polarization on overall efficiency.

Likewise, the recirculating power fraction, i.e., the ratio of power consumed to gross electrical produced, is another important factor in mirror feasibility evaluations and is intimately related to overall plant

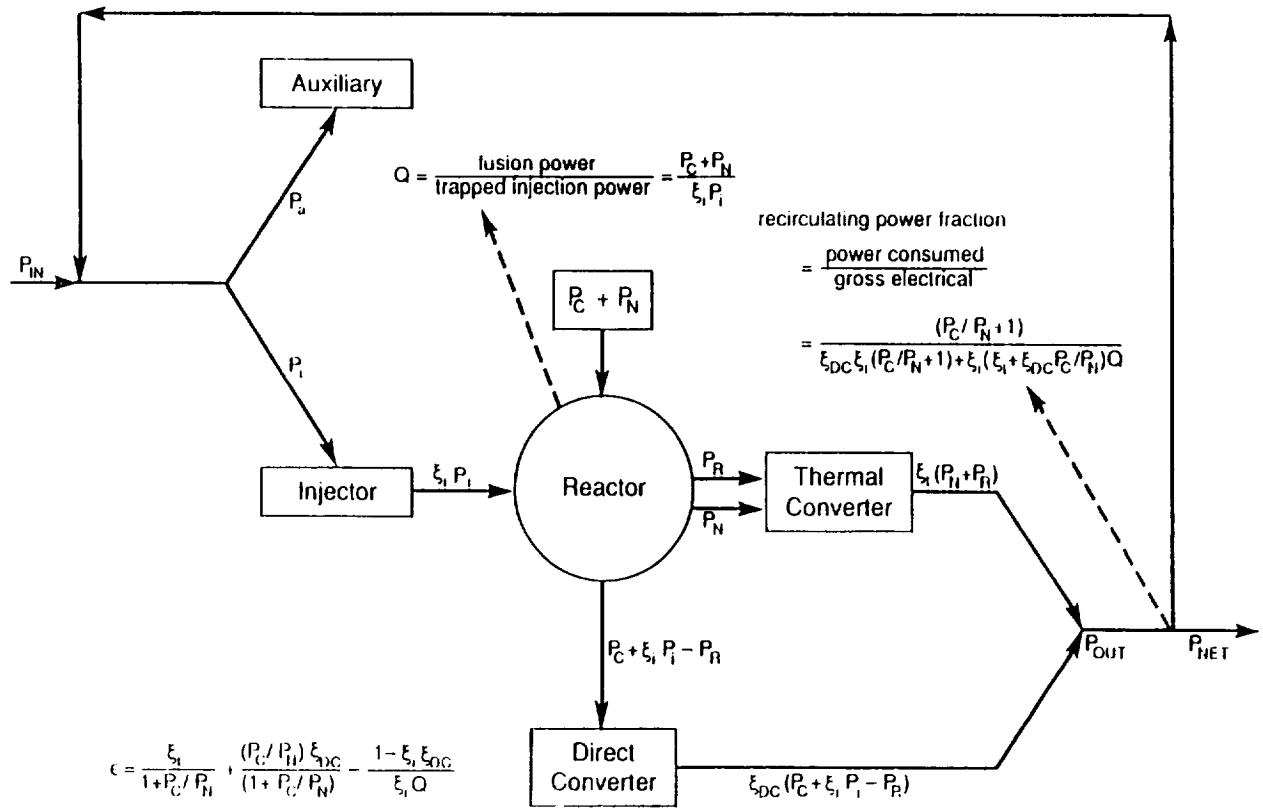
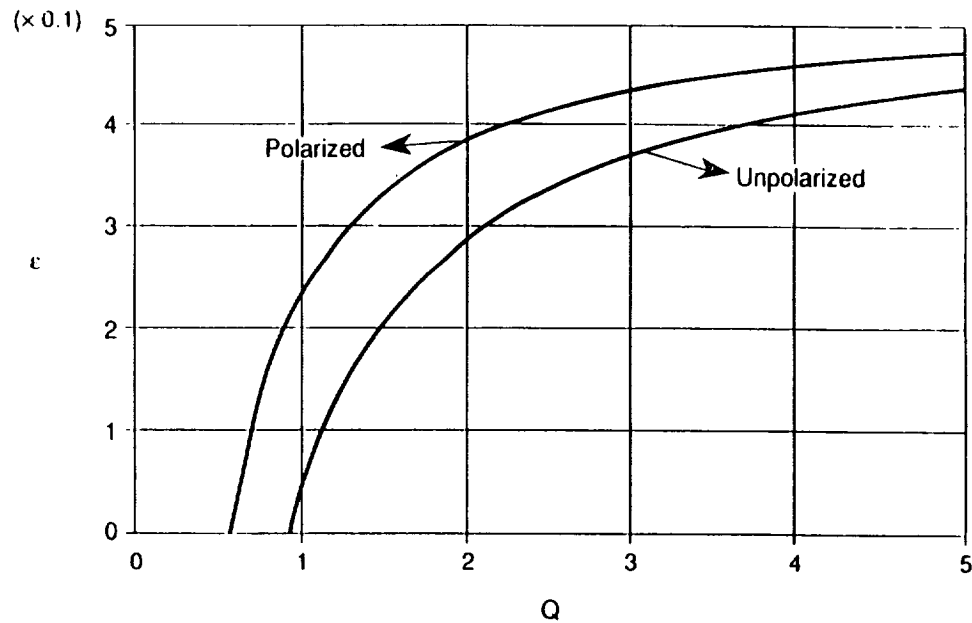


Fig. 13. Reactor schematic.


 Fig. 14. Overall thermal efficiency versus  $Q$ .

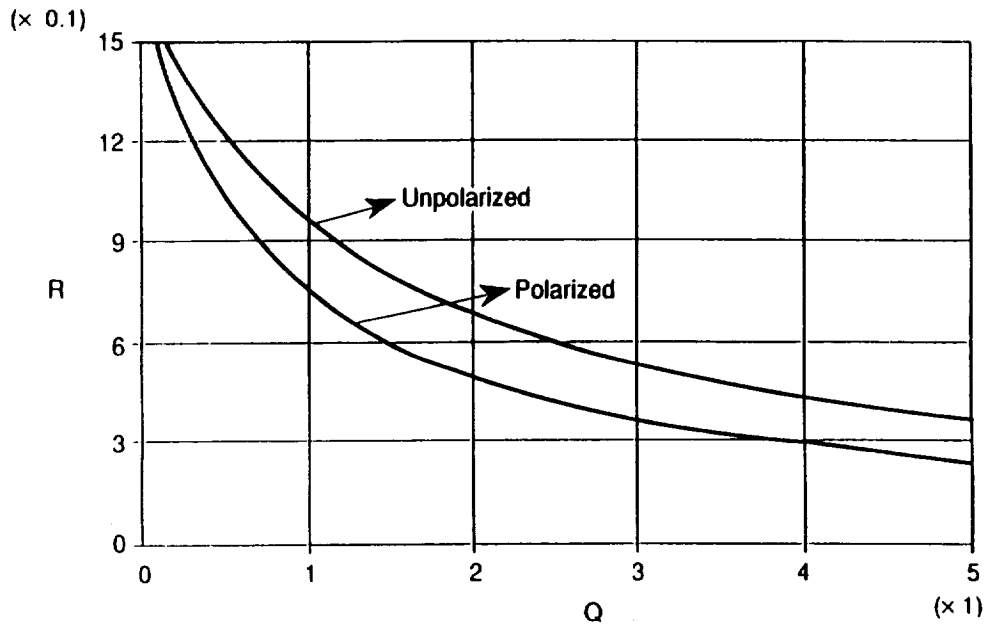


Fig. 15. Fractional recirculating power versus  $Q$ .

efficiency. Persistently high recirculating power requirements alone account for 13% of the total capital outlays estimated for the LMRD, and attempts to reduce this fraction are an important part of any cost reduction scheme. This fraction can be written as

$$R = \frac{\left(\frac{P_C}{P_N} + 1\right)}{\xi_{DC}\xi_i\left(\frac{P_C}{P_N} + 1\right) + \xi_i\left(\xi_i + \xi_{DC}\frac{P_C}{P_N}\right)Q}$$

and is shown in Fig. 15 for polarized and unpolarized injection and various  $Q$  values.

### Mirror Assessment

Given that power cost estimates for the standard mirror reactor run four times greater than the Wisconsin tokamak estimates and ten times greater than current fission costs, the mirror's future economic competitiveness depends on  $Q$  enhancement schemes. As demonstrated in Fig. 16, modest improvements in  $Q$  can significantly reduce the cost of power, and a  $Q$  enhancement of 5 is expected to bring mirror costs into competition with other future energy sources such as solar, coal-fired magnetohydrodynamics, and the fast breeder in the range of 50 to 70 mil/kW·h (Ref. 19).

While the  $Q$  enhancement of 1.63 found here for polarized nuclei falls short of these requirements, the potential for supplementing tandem or field-reversed mirror confinement with polarization holds some promise. Estimates for these other confinement schemes<sup>20</sup>

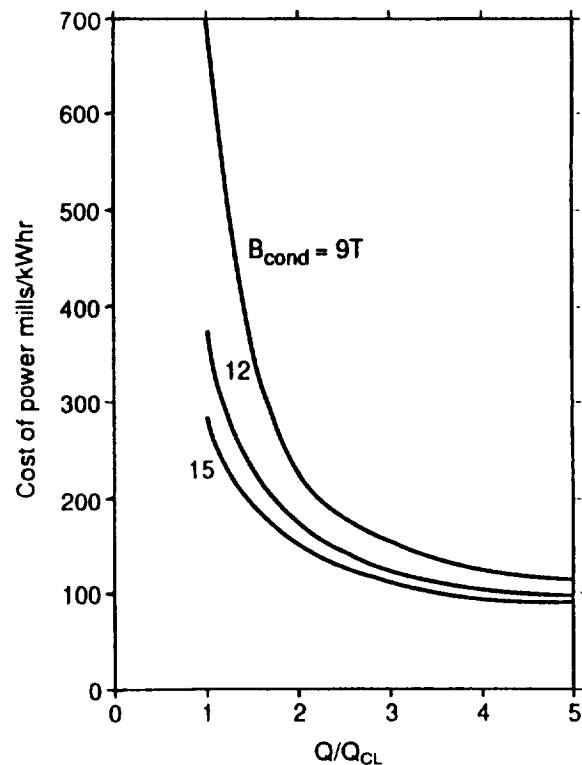


Fig. 16. Effect of  $Q$  enhancement on cost of power.

are in the  $Q$  enhancement range of 3 to 5, and, coupled with a low-cost polarization program, may provide a mirror  $Q = 5$  value or greater as required for future economic comparisons.

## SUMMARY AND CONCLUSIONS

The conceptual design of a mirror fusion reactor is analyzed to include polarized fuel. In discussing the various polarized designs, previous work has considered that the  $\sin^2 \vartheta$  angular distribution of fusion products might favor alpha-particle confinement and thus increase plasma heating. Compared with the classical unpolarized case, polarized fuel is found here to yield enhanced  $Q$  values (by a factor of 1.63). Estimated power is obtained from a Fokker-Planck representation that includes both direct and collisional losses. These improvements in alpha-particle confinement derive from polarized D-T nuclei that, in turn, produce a highly anisotropic alpha-particle source ( $\sin^2 \vartheta$ ) distribution. Following collisions, the alpha-particle products are tracked using a numerical solution and are found to maintain much of the high anisotropy initially fed to the reactor as polarized fuel.

To extend the model into higher collective modes of plasma behavior, nonlinear instabilities associated with the loss cone should be considered. A host of anomalous sources for alpha-particle losses can be represented, but nonlinear simulations may prove computationally difficult without resorting to more powerful scaling of variables or spectral techniques beyond the scope of this paper. For polarized fuel, the principal outcome of enhanced heating may encourage further progress not only for simple mirror designs but also for more elaborate geometries such as tandem or spheromak reactors.

## ACKNOWLEDGMENTS

The author thanks R. G. Mills, Princeton Plasma Physics Laboratory (PPPL), for suggesting the problem and PPPL for their hospitality.

## REFERENCES

1. L. W. ANDERSON, S. N. KAPLAN, R. V. PYLE, L. RUBY, A. S. SCHLACTER, and J. W. STEARNS, "Polarization of Fast Atomic Beams by 'Collisional Pumping': A Proposal for Production of Intense Polarized Beams," *Phys. Rev. Lett.*, **52**, 609 (1984).
2. R. M. KULSRUD, H. P. FURTH, E. J. VALEO, and M. GOLDBERGER, "Fusion Reactor Plasmas with Polarized Nuclei," *Phys. Rev. Lett.*, **49**, 1248 (1982).
3. J. J. LODDER, "On the Possibility of Nuclear Spin Polarization in Fusion Reactor Plasmas," *Phys. Lett.*, **98A**, 179 (1983).
4. R. M. KULSRUD, H. P. FURTH, E. J. VALEO, R. V. BUDNY, D. L. JASSBY, B. J. MICKLICH, D. E. POST, M. GOLDBERGER, and W. HAPPER, "Fusion Reactor Plasmas with Polarized Nuclei-II," *Proc. 9th Int. Conf. Plasma Physics and Controlled Nuclear Fusion Research*, Baltimore, Maryland, Vol. 2, p. 163, International Atomic Energy Agency (1983).
5. O. MITARAI, H. HASUYAMA, and Y. WAKUTA, "Spin Polarization Effect on Ignition Access Condition for D-T and D-He Tokamak Fusion Reactors," *Fusion Technol.*, **21**, 2265 (1992).
6. Y. WAKUTA, Y. WATANABE, S. URANO, O. MITARAI, and H. HASUYAMA, "Production of Intense Polarized Atoms and Its Applications to Tokamak Fusion Reactor," *Proc. 5th Int. Conf. Emerging Nuclear Energy Systems*, Karlsruhe, Germany, July 1989, p. 202.
7. E. BITTONI, A. FUBINI, and M. HAEGI, "Enhancement of Alpha Particle Confinement in Tokamaks in the Case of Polarized Deuterium and Tritium Nuclei," *Nucl. Fusion*, **23**, 830 (1983).
8. R. M. KULSRUD, E. J. VALEO, and S. C. COWLEY, "Physics of Spin Polarized Plasmas," *Nucl. Fusion*, **26**, 1443 (1986).
9. P. A. FINN, J. N. BROOKS, D. A. EHST, Y. GOHAR, R. F. MATTAS, and C. C. BAKER, "An Evaluation of Polarized Fuels in a Commercial Deuterium/Tritium Tokamak Reactor," *Fusion Technol.*, **10**, 902 (1986).
10. G. KAMELANDER and D. J. SIGMAR, "Evolution of Alpha-Particle Distribution in Burning Tokamaks Including Energy-Dependent and Transport Effects," *Physica Scripta*, **45**, 147 (1992).
11. D. ANDERSON and M. LISAK, "Scattering Losses of Alpha-Particles During Slowing Down in Magnetically Confined Plasmas," *Physica Scripta*, **26**, 333 (1982).
12. D. V. SIVUKHIN, "Coulomb Collisions in a Fully Ionized Plasma," *Reviews of Plasma Physics*, p. 93, Consultants Bureau, New York (1966).
13. D. ANDERSON, H. G. GUSTAVSSON, H. HAMNEN, and M. LISAK, "Alpha Particle Losses During Slowing Down in an Open-Field Line Fusion Plasma," *Nucl. Fusion*, **22**, 4038 (1982).
14. D. L. GALBRAITH and T. KAMMASH, "Alpha Particle Heating of Mirror Plasmas," *Proc. Symp. Technology of Controlled Thermonuclear Fusion Experiments and Engineering Aspects of Fusion Reactors*, Austin, Texas, November 20-22, 1972, p. 15, Texas Atomic Energy Research Foundation (1972).
15. R. G. MILLS, "Time-Dependent Behavior of Fusion Reactors," MATT-728, Princeton Plasma Physics Laboratory (1970).
16. T. KAMMASH, *Fusion Reactor Physics: Principles and Technology*, p. 35, Ann Arbor Science Publishers, Ann Arbor, Michigan (1976).



17. S. GLASSTONE and R. LOVBERG, *Controlled Thermonuclear Reactions: An Introduction to Theory and Experiment*, p. 18, R. Kreiger Publishing Company, Huntington, New York (1975).

18. "Standard Mirror Fusion Reactor Design Study," UCID-7644, Lawrence Livermore National Laboratory (1978).

19. T. KAWABE, "Present Status of Research on Open-Ended Fusion Systems," *Proc. Int. Symp. Physics in Open-Ended Fusion Systems*, University of Tsukuba, Ibaraki, Japan, 1980, p. 431.

20. R. W. CONN and G. L. KULCINSKI, "Fusion Reactor Design Studies," *Science*, **193**, 630 (1976).

